INTERNATIONAL JOURNAL OF CLIMATOLOGY
Int. J. Climatol. (2014)
Published online in Wiley Online Library
(wileyonlinelibrary.com) DOI: 10.1002/joc.4090

RMetS
Royal Meteorological Society

Short Communication

Multi-scalar influence of weather and climate on very large-fires in the Eastern United States

Renaud Barbero,[a]* John T. Abatzoglou,[a] Crystal A. Kolden,[a] Katherine C. Hegewisch,[a] Narasimhan K. Larkin[b] and Harry Podschwit[b]

[a] *Department of Geography, University of Idaho, Moscow, ID, USA*
[b] *Pacific Wildland Fire Sciences Laboratory, US Forest Service, Seattle, WA, USA*

ABSTRACT: A majority of area burned in the Eastern United States (EUS) results from a limited number of exceptionally large wildfires. Relationships between climatic conditions and the occurrence of very large-fires (VLF) in the EUS were examined using composite and climate-niche analyses that consider atmospheric factors across inter-annual, sub-seasonal and synoptic temporal scales. While most large-fires in the EUS coincided with below normal fuel moisture and elevated fire weather, VLF preferentially occurred during a long-term drought accompanied by more acute sub-seasonal drought realized through fuel moisture stress and elevated fire-weather conditions. These results were corroborated across the EUS, with varying influences of drought, fire danger and fire weather discriminating VLF from other large fires across different geographical regions. We also show that the probability of VLF conditioned by fire occurrence increases when long-term drought, depleted fuel moisture and elevated fire weather align. This framework illustrates the compounding role of different timescales in VLF occurrence and serves as a basis for improving VLF predictions with seasonal climate forecasts and climate change scenarios.

KEY WORDS very large-fires; Eastern United States; temporal scales; climate–fire linkages

Received 2 February 2014; Revised 23 May 2014; Accepted 28 May 2014

1. Introduction

The increasing frequency of very large wildfires across the United States and other regions of the globe has prompted the need to better examine the factors that contribute to their occurrence. Very large-fires (VLF) account for a large percentage of the total area burned, suppression costs and damages. While VLF result from a myriad of interacting factors, their increased prevalence in recent decades coinciding with changes in climate such as earlier spring snowmelt (Westerling *et al.*, 2006) and increased potential evaporation during the fire season (Morton *et al.*, 2013), has prompted the question of the influence of climate processes on VLF and whether changes in climate have enabled documented increases in VLF (Dennison *et al.*, 2014; Stravos *et al.*, 2014).

Wildfire is linked to atmospheric processes that occur on distinctly different time scales (Meyn *et al.*, 2007). While inter-annual moisture variability may enable a large wildfire season by increasing the landscape flammability, there is a need to resolve which temporal scales of climate variability best elucidate the conditions conducive to VLF, and how these factors vary across different fire regimes. The literature is currently inconclusive on this topic, with the occurrence of VLF attributed to inter-annual variability in moisture (Slocum *et al.*, 2010), sub-seasonal drought (<3 months) manifested through prolonged and depleted fuel moisture that increase landscape flammability (Stravos *et al.*, 2014), and to atmospheric processes on shorter timescales that may contribute to large fire growth such as critical fire-weather synoptic patterns (Pollina *et al.*, 2013). The 'Black Saturday' bushfires in Australia in February 2009 provide an example of the results of a confluence of multi-scalar weather and climate events, including preconditioning of fuels via abnormally low spring precipitation that promoted long-term drought (Cai *et al.*, 2009) and a capstone fire-weather event that brought fire-weather conditions unprecedented in the historic record (McCaw *et al.*, 2009). While most prior analyses have focused on a single timescale or process, the rarity of VLF suggests the role of compounding atmospheric factors in enabling and driving such fires.

While Hawbacker *et al.* (2013) showed that climatology of temperature and/or precipitation was the most important factor contributing to the spatial distribution of the largest 5% of fires in the United States, most prior studies in the Eastern United States (EUS) have examined climate–fire relationships at inter-annual timescales (e.g. Slocum *et al.*, 2010; Lafon and Quiring, 2012) expressed

* Correspondence to: R. Barbero, Department of Geography, University of Idaho, 875 Perimeter Drive MS 3021, Moscow, ID 83844-3021, USA.
E-mail: renaudb@uidaho.edu

© 2014 Royal Meteorological Society

primarily through inter-annual variability in moisture (e.g. Slocum *et al.*, 2010; Morton *et al.*, 2013). Several challenges in resolving macroscale climate–fire relationships in the EUS include widespread land cover fragmentation and use of prescribed fire in addition to a large proportion of human-ignited wildfires and poorly defined seasonality of wildfire occurrence (Malamud *et al.*, 2005). However, there is still a need to better understand how weather and climate contribute to VLF occurrence in the densely populated EUS due to direct risk to human life and property and widespread air quality impacts on dense population areas associated with the wildfire smoke emissions (Yue et al., 2013). Moreover, VLF often occur in unique habitat for numerous threatened and endangered species in isolated contiguous patches, such as the Okefenokee National Wildlife Refuge (Eadie, 1984; Yin, 1993) in Georgia and the Everglades National Park in Florida.

We used a satellite-derived fire perimeter database and a set of multi-temporal weather and climate variables to identify atmospheric factors that contribute to VLF occurrence in the EUS from 1984 to 2010. First, we examined whether there were differences between atmospheric conditions at inter-annual, sub-seasonal and synoptic timescales for VLF and other large fires, and what atmospheric timescales best distinguished VLF from other large fires across different regions on the EUS. Second, we used a climate-niche model spanning these three timescales to predict the conditional occurrence of VLF.

2. Dataset and methods

Fire perimeters for all large fires (>202 ha) east of 100°W in the contiguous United States (herein defined as EUS) were acquired for 1984–2010 from the Monitoring Trends in Burn Severity (MTBS; www.mtbs.gov). For each fire, we acquired the following attributes: (1) burned area for each burn severity class as quantified by MTBS, (2) latitude and longitude of the fire polygon centroid, and (3) discovery date of the fire. Within each fire, the 'unburned to low' class, which includes unburned islands within the fire perimeter, was excluded to better characterize the true area burned (Kolden *et al.*, 2012). We defined VLF as the largest 5% of fires in the MTBS database by area burned (>∼3000 ha). Large fires (hereafter LF) were defined as the remaining 95% of fires in the MTBS data set. This threshold is purely statistical in nature; however, results were not sensitive to selecting a lower threshold (e.g. 90%). A total of 231 VLF accounted for more than 52% of the total area burned in the data set (Table 1).

Previous studies in the western United States have analysed macroscale climate–fire relationships using geopolitical boundaries, fire management units or ecoregion scales (e.g. Westerling *et al.*, 2003; Littell *et al.*, 2009; Abatzoglou and Kolden, 2013). However, Morton *et al.* (2013) noted that the seasonality of fires in the EUS was very heterogeneous and that climate–fire relationships were particularly difficult to generalize, given large within-region climate variability and ecosystem diversity. Coarser scale analyses may increase the signal-to-noise ratio and heterogeneity in fuel types involved as compared with more fine-scale analyses; however, finer-scale analyses result in the statistical challenge of decreased sample size, particularly when dealing with rare events such as VLF.

We identified geographic hot-spots of VLF activity as a means of defining regions of the EUS for subsequent analysis. We clustered VLF centroid locations by applying the *k*-means clustering algorithm iteratively to define *k* centroids while reducing sensitivity to the initial randomly selected cluster centroid. The optimal classification yielded six clusters (Figure 1) driven by similar climate anomalies (e.g. Trigo *et al.*, 2013). Large fires located within 500 km of a VLF cluster were included in that cluster (Figure 1). We excluded LF with discovery dates within ±7 days of a VLF discovery date for each cluster to avoid confounding signals as VLF and LF often occur synchronously within a region when conditions are prone to a VLF.

We used several variables operating at three distinct and nearly orthogonal timescales to capture inter-annual, sub-seasonal and synoptic variability associated with each wildfire. While most prior climate–fire studies have used variables such as temperature and precipitation given their widespread availability, we focus on a set of integrated variables that incorporate a consortium of surface meteorological variables over distinct time periods. The Palmer drought severity index (PDSI) was used to assess low-frequency inter-annual moisture variability. The PDSI was computed using temperature and precipitation data from Parameter-Elevation Regressions on Independent Slopes Model (PRISM, Daly *et al.*, 2008) at 800-m resolution following the methods of Kangas and Brown (2007). The Energy Release Component (ERC) of the US National Fire Danger Rating System (NFDRS; Deeming *et al.*, 1977) was used to estimate the influence of sub-seasonal timescales as it is a cumulative, hybrid weather-climate metric that indicates potential heat energy released at the flaming front. The Fosberg fire weather index (FFWI; Fosberg, 1978) was used to estimate daily synoptic timescales

Table 1. MTBS fire statistics for each region. The table provides the number of large fires (LF) and very large-fires (VLF) in each cluster as well as the percent of area burned by VLF (ABVLF).

	EUS	Appalachians	Northern Minnesota	East coast	Great Plains	Texas–Louisiana	Florida
#LF	3607	642	251	267	727	436	1384
#VLF	231	44	24	9	79	14	61
%ABVLF	52	41	60	47	46	17	44

© 2014 Royal Meteorological Society

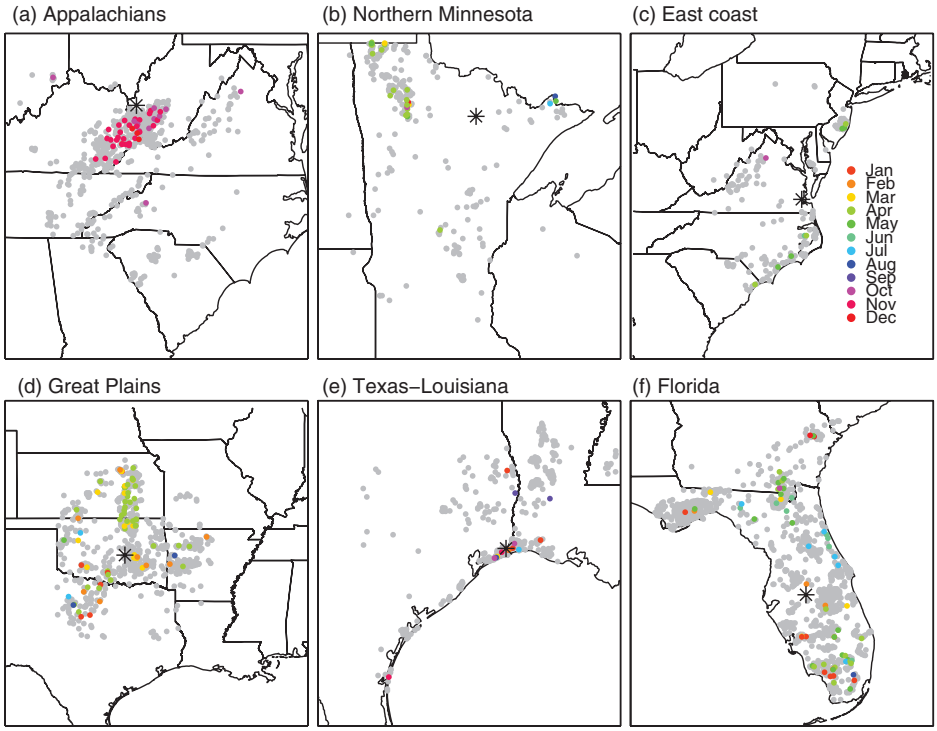

Figure 1. Spatio-temporal occurrences of VLF in each cluster. VLF clusters are computed from the *k*-means algorithm using longitudes and latitudes of VLF. Colour dots depict VLF while grey dots indicate LF. The asterisk symbol within each cluster indicates VLF centroid. Both VLF and LF located further than 500 km from the cluster centroid were excluded.

as it captures short-term impact of weather on wildfire potential through wind events and heat waves (Fosberg, 1978; Cary *et al.*, 2009). We considered FFWI, over other fire danger metrics, to differentiate the relative influence of sub-seasonal and synoptic timescales given the weak correlation ($R^2 = 0.06$) between ERC and FFWI. Using other variables to define sub-seasonal such as the Duff Moisture Code and synoptic variability such as the Burning index or *F*-index (Sharples *et al.*, 2009) did not improve our results. Daily ERC and FFWI values were computed from the gridded surface meteorological dataset of Abatzoglou (2013) at 4-km spatial and daily temporal resolution. To account for the spatial heterogeneity in predictor variables across the EUS, we converted ERC and PDSI into percentiles and daily FFWI into deseasonalized standardized anomalies. Fire danger and PDSI data were extracted for each fire by taking the grid cell collocated with each fire centroid.

We examined lead-lag composites of the three variables relative to the discovery dates for both VLF and LF. We considered a 16-day window (5 days before to 10 days after the discovery date) for FFWI, a 61-day window (30 days before to 30 days after discovery date) for ERC and a 21-month window (18 months before to 2 months after discovery month) for PDSI, spanning the previous growing season (May to September in the EUS) of any fire, including fires that occurred at the end of the year. The 95% confidence intervals of the composite means were computed using 1000 bootstrapped datasets.

On the basis of the aforementioned exploratory composite analysis, we examined the climate-niche of VLF across the three-dimensional climate space spanned by PDSI, ERC and FFWI. The climate-niche considers data from these three variables over a specific temporal window. It is challenging to define an optimal window over which an individual variable may influence the likelihood of a fire becoming a VLF particularly as some fires might burn only over a few days, and others over a few month period as seen during the Bugaboo Scrub fire in Georgia in 2007. To better constrain our choice of temporal window, we used the Smartfire v2 database that provides estimates of daily fire growth and emissions for MTBS fires from 2003 to 2010 (Raffuse *et al.*, 2012). We further subsampled from these fires by examining only fires where the discovery date (defined by MTBS) and initial growth day (defined by SmartFire v2) were less than 7 days apart. An average of more than 80% of the total burned area for VLF occurred over the first 10 days post-ignition (Figure 2). On the basis of these results, we defined a three-dimensional climate-niche by considering (1) inter-annual variability represented by PDSI coincident to the month of fire, (2) sub-seasonal variability, represented by ERC averaged over a 21-day window, spanning 10 days before to 10 days after the discovery date of the fire and (3) synoptic variability represented by the maximum consecutive 3-day FFWI over the 10 days post-discovery. We used a 10-day window following the discovery date as a time period that encapsulates a primary growth period of most large fires (Figure 2).

We considered a climate-niche model demarcated by thresholds for each variable. The forecasted distribution of VLF is represented by a binary matrix of VLF forecasts

© 2014 Royal Meteorological Society

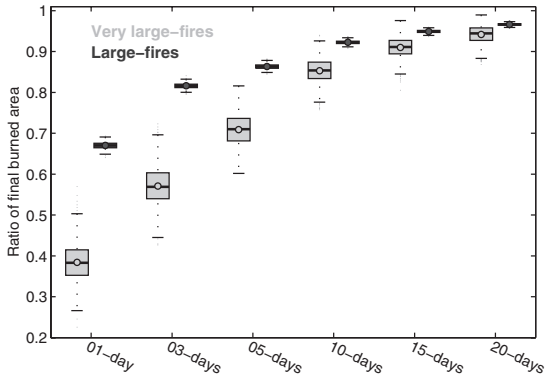

Figure 2. Ratio of final burned area for large-fires (dark grey) and very large-fires (light grey) in the EUS from Smartfire v2 database (2003–2010) as a function of the number of days post-ignition. The confidence intervals of the composites are computed using 1000 bootstrapped datasets. The box indicates the interquartile range of the composites and the line with the circle shows the median obtained from the bootstrapped datasets.

($\mathrm{VLF_{fct}}$) in each climate-niche (i, j, k),

$$\mathrm{VLF_{fct}}(i,j,k) = \begin{cases} 1 & \text{if FFWI} \geq i,\ \text{ERC} \geq j,\ \text{PDSI} \leq k \\ 0 & \text{otherwise} \end{cases} \quad (1)$$

where climate-niche demarcations are defined by the thresholds $i = 0$, 1, 2 standard deviations for deseasonalized FFWI and j, $k = 0, 5, \ldots, 95$ percentile for both ERC and PDSI. We computed VLF probability given fire occurrence in each climate-niche using a Laplace's correction. This model was evaluated using the observed distribution of VLF and LF. We assessed the skill of each climate-niche model using the Heidke Skill Score (HSS) from a contingency table of the joint frequency distributions of $\mathrm{VLF_{fct}}$ and VLF observations (Wilks, 2006), where a perfect forecast has HSS = 1, and a forecast with no skill or skill below that of a random forecast has HSS = 0 and HSS < 0, respectively. The climate-niche associated with the highest HSS (Sohn and Park, 2008) is reasoned to provide an indication on the confluence of synoptic, sub-seasonal and inter-annual variability associated with VLF occurrence.

3. Results

VLF clustering yielded six regions across the EUS: Appalachians, Northern Minnesota, East Coast, Great Plains, Texas–Louisiana and Florida (Figure 1), generally adhering to large-scale ecoregions of the EUS (e.g. Bailey *et al.*, 1994). The seasonal windows during which VLF occurred were more constrained than for LF, suggesting that seasonal factors facilitate VLF occurrence (not shown). VLF typically occurred immediately following the annual nadir in precipitation when fuels are driest and most available. For example, nearly all VLF in the Appalachians and most of the burned area occurred during a relatively short period (~1 month) at the end of October when the accumulation of fine fuels associated with the autumn leaf fall combine with low precipitation and relative humidity to support fire spread (Maingi and Henry, 2007). Table 1 indicates that VLF accounted for 40–60% of the total area burned in all regions except in Texas–Louisiana (~17%). Correlations between the square root of VLF burned area and the square root of total fire burned area at inter-annual timescales (computed only when at least one VLF occurred in a given year) were strongly correlated ($R^2 = 0.9$ at the EUS scale), in agreement with the findings of Stravos *et al.* (2014) in the western United States.

An example of inter-annual, intra-seasonal and synoptic signals for the Bugaboo Scrub Fire that began in April 2007 and burned 81 902 ha in Georgia and Florida is provided in Figure 3. The fire occurred during a long-term drought (Figure 3(a)) and under exceptional prolonged fire danger with ERC exceeding the historical 95th percentile for several weeks prior to and nearly 30 days following the fire discovery date (Figure 3(b)). Superposed on the long-term and intra-seasonal drought were period of significant fire weather as viewed through FFWI (Figure 3(c)). Large fire runs (Figure 3(b)) after fire discovery coincided with high ERC but also consecutive days with FFWI $>2.5\sigma$ when outflow from the subtropical storm Andrea brought high winds and low humidity that likely facilitated fire spread (Wildfire Hazard Mitigation Annex). Although the signature of inter-annual to synoptic factors varies across VLF, we hypothesize that combinations of these factors create conditions conducive for VLF.

Significantly higher fire danger and fire-weather conditions and lower PDSI were observed during VLF compared with LF when considering all fires in EUS (Figure 4). PDSI was significantly lower than normal for VLF, and lower than that of LF in all clusters except in Texas–Louisiana. No significant longer-term antecedent signals in PDSI evident in the previous growing season were observed in any of the clusters suggesting fuel-limited climate–fire relationships seen in other regions were not present. This is not surprising, given the prevailing forest dominated biomes and high levels of annual precipitation across the EUS outside of the western Great Plains. Longer-term drought stress is thus reasoned to be critical for depleting fuel moistures of large diameter trees and lowering of the water table in swamp forests and wetlands allowing these fuels to be receptive to fire during protracted moisture deficits (Watts and Kobziar, 2013).

ERC was significantly higher during VLF than LF consistent with increased receptiveness of landscapes to widespread fire activity when fuel moistures are low (Figure 4, middle panels). However, relationships varied at regional scales, with significantly higher ERC for VLF than LF in the East Coast, Florida and Northern Minnesota regions. The occurrence of prolonged and elevated ERC might be expected with a blocking ridge aloft (Pollina *et al*, 2013), or other persistent atmospheric regimes that bring anomalously warm and dry conditions. Similarly,

© 2014 Royal Meteorological Society

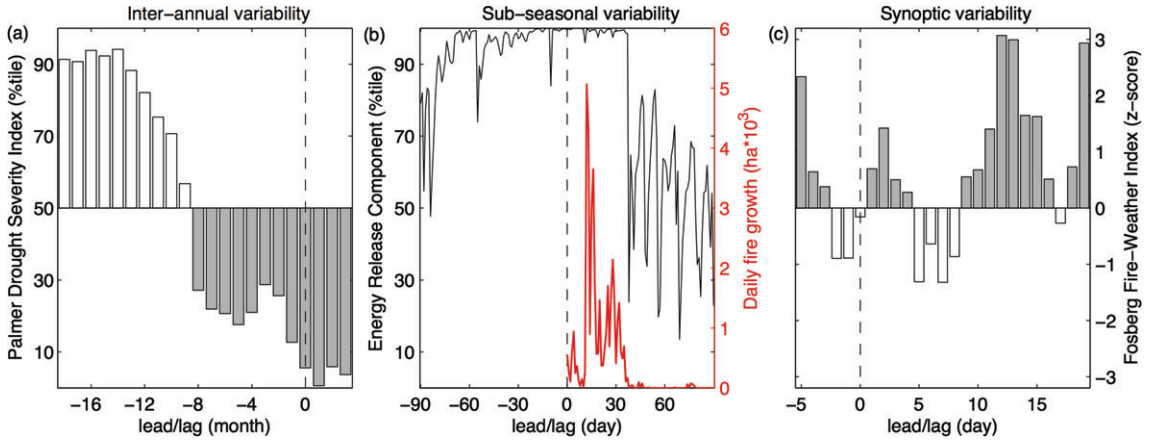

Figure 3. (a) Inter-annual variability represented by PDSI, (b) sub-seasonal variability represented by ERC and (c) synoptic variability represented by FFWI associated with the 'Bugaboo Scrub Fire' (renamed 'Big Turnaround Complex') in Georgia which started in 16 April 2007 and burned 81 902 ha. Daily fire growth estimated from the SmartFire v2 data is shown by the solid line in (b). The vertical dashed line in each plot represents the fire discovery date reported in MTBS.

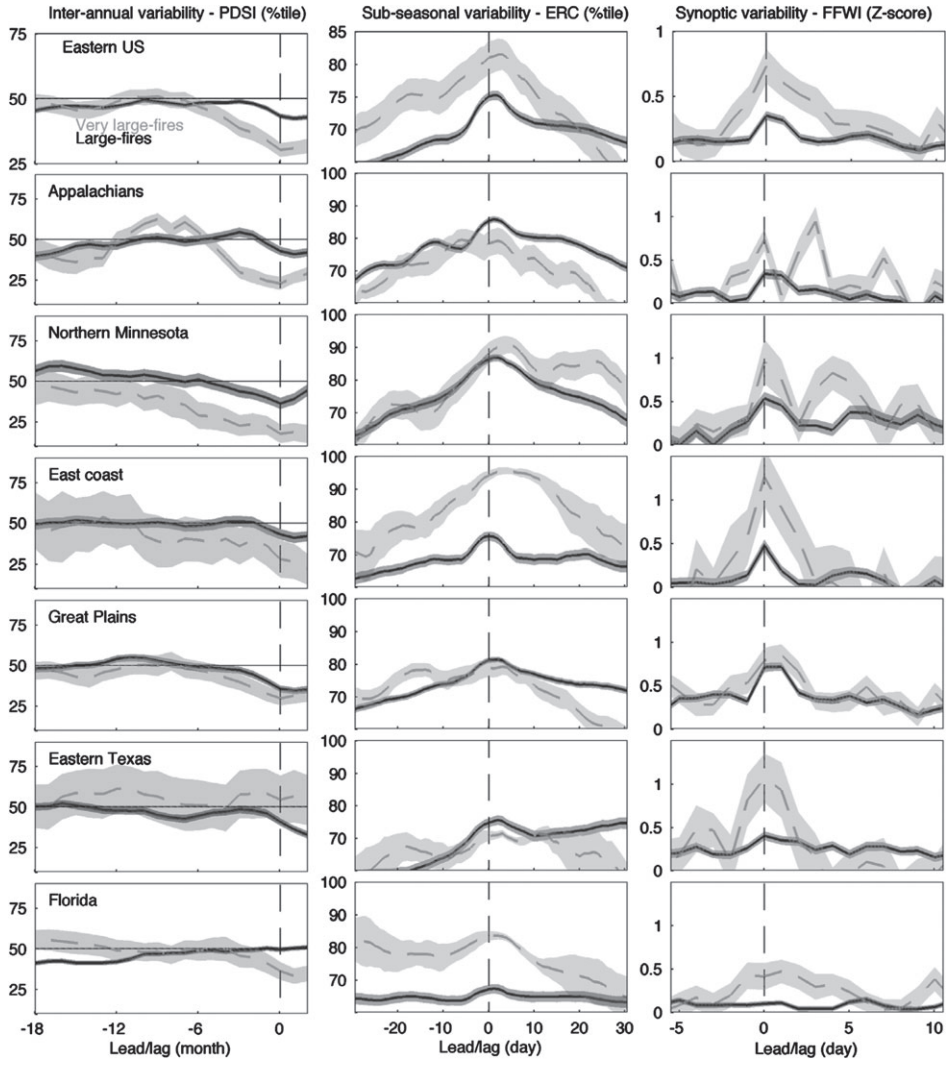

Figure 4. Left panels: lead/lag composites of PDSI relative to the discovery month of LF (dark grey) and VLF (light grey) at the EUS scale (first line) and at the regional scale. Middle panels: same except for ERC (expressed as percentiles) except the lead/lag is relative to fire discovery day. Right panels: same except for FFWI (expressed as standardized anomalies). The 95% confidence intervals of the composite means are computed using 1000 bootstrapped datasets. The envelope of confidence indicates the 2.5 and 97.5 percentile of the composite means obtained from the bootstrapped datasets.

© 2014 Royal Meteorological Society

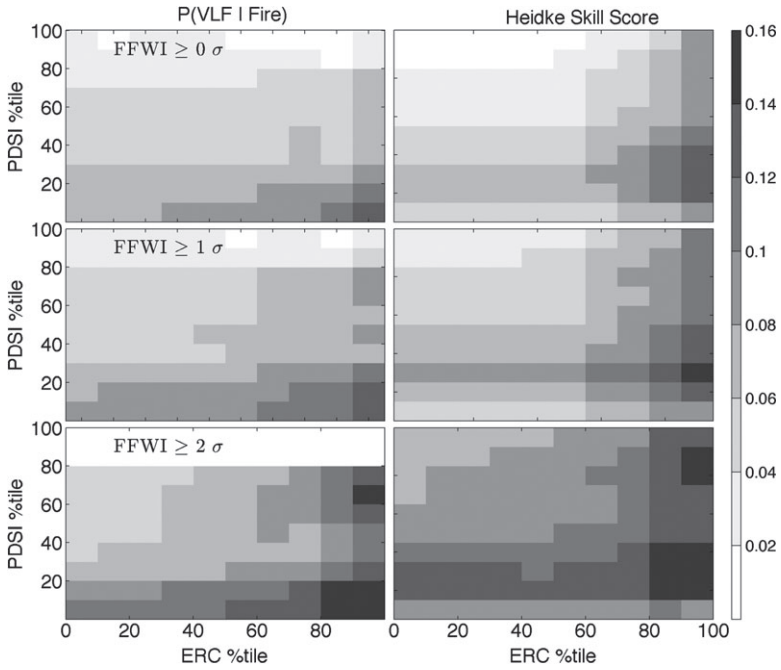

Figure 5. Left panels: very large-fire probability given fire occurrences as a function of FFWI (>0, >1, >2), ERC and PDSI thresholds from 0 to 95 with a 5% increment. ERC (x-axis) was averaged over 21 days (10 days before to 10 days after the discovery date of fire), PDSI corresponds to PDSI during the month of fire (y-axis) and FFWI corresponds to the maximum consecutive 3-day FFWI over 10 days post-discovery date. Right panels: HSS optimization for VLF forecasts. Score is calculated for various thresholds of PDSI, ERC and FFWI as in the left panels. The colour bar refers to both left and right panels.

FFWI was significantly higher than normal concurrent with and in the week following the discovery date during VLF (Figure 4, right panels). This is consistent with other studies that showed that fire-weather conditions were important for LF occurrences in United States (e.g. Brotak and Reifsnyder, 1977).

Probabilities for three-dimensional climate-space for VLF conditioned by fire occurrence for the EUS are shown in Figure 5 (left panels). VLF probability increases in conjunction with an increased FFWI and ERC and decreased in PDSI, and these findings are generally robust at the regional level (not shown). The HSS using the same climate-space are displayed on Figure 5 (right panels). Combining the three timescales results in appreciable skill, especially during the confluence of low PDSI and high ERC and FFWI. Note the lack of a single dimension or variable that resolves VLF likelihood. For example, the presence of critical fire-weather conditions in the absence of seasonal or long-term drought yields nominal skill. The climate-niche associated with the highest HSS at the EUS scale was defined by PDSI <25th percentile, ERC >90th percentile and FFWI >2σ (Table 2). Similar relationships were found at the regional scale, with the multivariate approach including all variables resulting in increased HSS values and an increase in the VLF probability given fire occurrence for all regions except in Texas–Louisiana. This simple binary forecast based on three timescales relative to the fire event scale shows that alignment of three time scales yields optimal forecast skill in EUS and demonstrates the uniqueness of the weather-climate continuum associated with VLF.

Table 2. Combination of synoptic (FFWI), sub-seasonal (ERC) and inter-annual (PDSI) variables thresholds associated with the highest HSS. All indices are expressed as percentiles except FFWI that is expressed as standardized anomalies. A cell is blank when the variable does not increase the HSS. The last column indicates the VLF probability given fire occurrence under the climatic conditions defined by the thresholds.

Region	FFWI	ERC	PDSI	HSS	VLF:total fires
Eastern United States	>2	>85	<25	0.17	0.27
Appalachians	>2	>80	<30	0.30	0.33
Northern Minnesota	>2	>95	<40	0.38	0.45
East Coast	>2	>85	<35	0.26	0.27
Great Plains	>2	>80	<40	0.08	0.23
Texas–Louisiana	>2	>85		0.15	0.03
Florida	>2	>85	<20	0.27	0.58

4. Conclusions

VLF in the EUS generally occur during long-term drought, and more pronounced sub-seasonal drought and fire-weather conditions than other LF, consistent with the analysis of Stravos *et al.* (2014) for the western United States. These results reinforce the notion that weather and climate play important roles in the occurrence of VLF and may supersede the capacity of fire suppression to control fire growth under such conditions. Further studies that can better elucidate the impact of daily or sub-daily weather conditions on daily fire growth of VLF are needed to refine such analysis, therein requiring high quality fire progression maps estimated from satellites

© 2014 Royal Meteorological Society

(e.g. Parks, 2014). While our study explicitly focused on atmospheric influences, other factors such as road or population density, multiple ignitions coupled with inadequate suppression resources, or fire-regimes associated with stand replacement vegetation are likely important factors that explain why some fires became VLF. Thus, while the alignment of inter-annual, intra-seasonal and synoptic atmospheric processes help enable VLF occurrence, they are not a sufficient or necessary condition for VLF.

The uniqueness of the climate-niche conducive to VLF occurrence may refine seasonal fire prediction efforts. For example, understanding how large-scale climate variability such as El-Niño Southern Oscillation (Beckage *et al.*, 2003) impacts both sub-seasonal fire danger and critical fire-weather events may improve seasonal VLF forecasts. The superimposition of synoptic, sub-seasonal and inter-annual forcing should also be considered in long-term climate change projections as changes in the occurrence of long-term drought, sub-seasonal fuel moisture and critical fire-weather conditions under enhanced greenhouse forcing could alter the frequency and geographic distribution of VLF.

Acknowledgements

We acknowledge the helpful feedback from three anonymous reviewers. This research was supported by the Joint Fire Science Program award number 11-1-7-4.

References

Abatzoglou JT. 2013. Development of gridded surface meteorological data for ecological applications and modeling. *Int. J. Climatol.* **33**: 121–131, DOI: 10.1002/joc.3413.

Abatzoglou JT, Kolden CA. 2013. Relationships between climate and macroscale area burned in the western United States. *Int. J. Wildland Fire* **22**: 1003–1020, DOI: 10.1071/WF13019.

Bailey RG, Avers PE, King T, McNab WH. 1994. *Ecoregions and Subregions of the United States (map)*(supplementary table of map unit descriptions compiled and edited by McNab WH and Bailey RG). U.S. Department of Agriculture–Forest Service scale 1:7,500,000: Washington, DC.

Beckage B, Platt WJ, Slocum MG, Panko B. 2003. Influence of the El Niño-Southern Oscillation on the fire regimes of the Florida Everglades. *Ecology* **84**: 3124–3130.

Brotak EA, Reifsnyder WE. 1977. An investigation of the synoptic situations associated with major wildland fires. *J. Appl. Meteorol.* **16**(9): 867–870.

Cai W, Cowan T, Raupach M. 2009. Positive Indian Ocean dipole events precondition southeast Australia bushfires. *Geophys. Res. Lett.* **36**: L19710, DOI: 10.1029/2009GL039902.

Cary GJ, Flannigan MD, Keane RE, Bradstock RA, Davies ID, Lenihan J, Li C, Logan KA, Parsons RA. 2009. Relative importance of fuel management, ignition management and weather for area burned: evidence from five landscape-fire-succession models. *Int. J. Wildland Fire* **18**: 147–156.

Daly C, Halbleib M, Smith JI, Gibson WP, Doggett MK, Taylor GH, Curtis J, Pasteris PP. 2008. Physiographically sensitive mapping of climatological temperature and precipitation across the conterminous United States. *Int. J. Climatol.* **28**: 2031–2064.

Deeming JE, Burgan RE, Cohen JD. 1977. The National Fire-Danger Rating System – 1978 USDA Forest Service. General Technical Report No. INT-39, Intermountain Forest and Range Experiment Station, Ogden, UT.

Dennison PE, Brewer SC, Arnold JD, Moritz MA. 2014. Large wildfire trends in the western United States, 1984–2011. *Geophys. Res. Lett.* **41**: 2928–2933, DOI: 10.1002/2014GL059576.

Eadie JR. 1984. History of Okefenokee National Wildlife Refuge. In *The Okefenokee Swamp: Its Natural History, Geology, and Geochemistry*, Cohen AD, Casagrande DJ, Andrejko MJ, Best GR (eds). Wetland Surveys: Los Alamos, NM, 2–4.

Fosberg MA. 1978. Weather in wildland fire management: the fire weather index. In *Proceedings of the Conference on Sierra Nevada Meteorology*, South Lake Tahoe, CA, 19–21 June 1978, 1–4.

Hawbacker TJ, Radeloff VC, Stewart SI, Hammer RB, Keuler NS, Clayton MK. 2013. Human and biophysical influences on fire occurrence in the United States. *Ecol. Appl.* **23**(3): 565–582.

Kangas RS, Brown TJ. 2007. Characteristics of US drought and pluvials from a high-resolution spatial dataset. *Int. J. Climatol.* **27**(10): 1303.

Kolden CA, Lutz JA, Key CH, Kane JT, van Wagtendonk JW. 2012. Mapped versus actual burned area within wildfire perimeters: characterizing the unburned. *For. Ecol. Manage.* **286**: 38–47.

Lafon CW, Quiring SM. 2012. Relationships of fire and precipitation regimes in temperate forests of the Eastern United States. *Earth Interact.* **16**: 11, DOI: 10.1175/2012EI000442.1.

Littell JS, McKenzie D, Peterson DL, Westerling AL. 2009. Climate and wildfire area burned in western U. S. ecoprovinces, 1916–2003. *Ecol. Appl.* **19**: 1003–1021.

Maingi JK, Henry MC. 2007. Factors influencing wildfire occurrence and distribution in eastern Kentucky, USA. *Int. J. Wildland Fire* **16**(1): 23–33.

Malamud BD, Millington JDA, Perry GLW. 2005. Characterizing wildfire regimes in the USA. *Proceedings of the National Academy of Sciences of the United States of America*. **102**(13): 4694–4699.

McCaw L, Mills G, Sullivan A, Hurley R, Ellis P, Matthews S, Plucinski M, Pippen B, Boura J. 2009. Fire behaviour investigation. In *Victorian 2009 Bushfire Research Response Final Report*. Bushfire CRC: Victoria, Australia, 63pp.

Meyn A, White PS, Buhk C, Jentsch A. 2007. Environmental drivers of large, infrequent wildfires: the emerging conceptual model. *Prog. Phys. Geogr.* **31**: 287–312.

Morton DC, Collatz GJ, Wang D, Randerson JT, Giglio L, Chen Y. 2013. Satellite-based assessment of climate controls on U.S. burned area. *Biogeosciences* **10**: 247–260, DOI: 10.5194/bg-10-247-2013.

Parks SA. 2014. Mapping day-of-burning with coarse-resolution satellite fire-detection data. *Int. J. Wildland Fire* **23**: 215–223, DOI: 10.1071/WF13138.

Pollina JB, Colle BA, Charney JJ. 2013. Climatology and meteorological evolution of major wildfire events over the Northeast United States. *Weather Forecast.* **28**: 175–193.

Raffuse S, Du Y, Larkin N, Lahm P. 2012. Development of the 2008 wildland fire National Emissions Inventory. In *20th International Emissions Inventory Conference*, Tampa, FL, 13–16 August, 12 pp.

Sharples JJ, McRae RHD, Weber RO, Gill AM. 2009. A simple index for assessing fire danger rating. *Environ. Model. Softw.* **24**(6): 764–774.

Slocum MG, Beckage B, Platt WJ, Orzell SL, Taylor W. 2010. Effect of climate on wildfire size: a cross-scale analysis. *Ecosystems* **13**: 828–840.

Sohn KT, Park SM. 2008. Guidance on the choice of threshold for binary forecast modeling. *Adv. Atmos. Sci.* **25**(1): 83–88.

Stravos EN, Abatzoglou JT, Larkin NK, McKenzie D, Steel EA. 2014. Very large-fires: an analysis of climatic factors associated with very large wildfires in the western contiguous United States. *Int. J. Wildland Fire* (in press).

Trigo RM, Sousa PM, Pereira MG, Rasilla D, Gouveia CM. 2013. Modelling wildfire activity in Iberia with different atmospheric circulation weather types. *Int. J. Climatol.*, DOI: 10.1002/joc.3749.

Watts AC, Kobziar LN. 2013. Smoldering combustion and ground fires: ecological effects and multi-scale significance. *Fire Ecol.* **9**: 124–132, DOI: 10.4996/fireecology.0901.

Westerling AL, Gershunov A, Brown TJ, Cayan DR, Dettinger DM. 2003. Climate and wildfire in the western United States. *Bull. Am. Meteorol. Soc.* **84**: 595–604.

Westerling AL, Hidalgo HG, Cayan DR, Swetnam TW. 2006. Warming and earlier spring increases Western U.S. forest wildfire activity. *Science* **313**: 940–943, DOI: 10.1126/science.1128834.

Wilks DS. 2006. *Statistical Methods in the Atmospheric Sciences*, 2nd edn. Academic Press: Burlington, VT, 627pp

Yin ZY. 1993. Fire regime of the Okefenokee Swamp and its relation to hydrological and climatic conditions. *Int. J. Wildland Fire* **3**: 229–240.

Yue X, Mickley LJ, Logan JA, Kaplan JO. 2013. Ensemble projections of wildfire activity and carbonaceous aerosol concentrations over the western United States in the mid-21st century. *Atmos. Environ.* **77**: 767–780, DOI: 10.1016/j.atmosenv.2013.06.003.

© 2014 Royal Meteorological Society